

SPECTROSCOPIC CONFIRMATION OF A $Z = 6.740$ GALAXY BEHIND THE BULLET CLUSTER*

MARUŠA BRADAČ¹, EROS VANZELLA², NICHOLAS HALL¹, TOMMASO TREU^{3,x}, ADRIANO FONTANA⁴, ANTHONY H. GONZALEZ⁵, DOUGLAS CLOWE⁶, DENNIS ZARITSKY⁷, MASSIMO STIAVELLI⁸, BENJAMIN CLÉMENT⁷

Draft version July 13, 2018

ABSTRACT

We present the first results of our spectroscopic follow-up of $6.5 < z < 10$ candidate galaxies behind clusters of galaxies. We report the spectroscopic confirmation of an intrinsically faint Lyman Break Galaxy (LBG) identified as a $z_{850\text{LP}}$ -band dropout behind the Bullet Cluster. We detect an emission line at $\lambda = 9412\text{\AA}$ at $> 5\text{-}\sigma$ significance using a 16hrs long exposure with FORS2 VLT. Based on the absence of flux in bluer broad-band filters, the blue color of the source, and the absence of additional lines, we identify the line as Lyman- α at $z = 6.740 \pm 0.003$. The integrated line flux is $f = (0.7 \pm 0.1 \pm 0.3) \times 10^{-17} \text{erg/s/cm}^2$ (the uncertainties are due to random and flux calibration errors, respectively) making it the faintest Lyman- α flux detected at these redshifts. Given the magnification of $\mu = 3.0 \pm 0.2$ the intrinsic (corrected for lensing) flux is $f^{\text{int}} = (0.23 \pm 0.03 \pm 0.10 \pm 0.02) \times 10^{-17} \text{erg/s/cm}^2$ (additional uncertainty due to magnification), which is $\sim 2 - 3$ times fainter than other such measurements in $z \sim 7$ galaxies. The intrinsic $H_{160\text{W}}$ -band magnitude of the object is $m_{H_{160\text{W}}}^{\text{int}} = 27.57 \pm 0.17$, corresponding to $0.5L^*$ for LBGs at these redshifts. The galaxy is one of the two sub- L^* LBG galaxies spectroscopically confirmed at these high redshifts (the other is also a lensed $z = 7.045$ galaxy), making it a valuable probe for the neutral hydrogen fraction in the early Universe.

Subject headings: galaxies: high-redshift — Gravitational lensing: strong — Galaxies: clusters: individual — dark ages, reionization, first stars

1. INTRODUCTION

The epoch of reionization, which marks the end of the “Dark Ages” and the transformation of the universe from opaque to transparent, is poorly understood. It is thought that $z > 6$ faint proto-galaxies were responsible for this transformation, but recent observations of $z \gtrsim 7$ objects (e.g., Robertson et al. 2010 for a review) complicate that scenario. Finding robust samples of sources, representative of the population contributing a significant amount of energetic photons, is crucial.

Wide Field Camera 3 (WFC3) on HST enables a preliminary identification of such galaxies. Sub-

stantial progress has been made in detecting $z \gtrsim 7$ galaxies using the dropout technique (Steidel et al. 1996), both in blank fields (HUDF, Candels, e.g., Bouwens et al. 2012, Oesch et al. 2012, Finkelstein et al. 2012, McLure et al. 2011), and behind galaxy clusters (e.g., Kneib et al. 2004, Egami et al. 2005, Bradley et al. 2012, Richard et al. 2011, Zheng et al. 2012, Zitrin et al. 2012 and references therein). One of the most obvious limitations of the dropout technique, however, is that unambiguously confirming the object’s redshift usually requires spectroscopic follow-up. This is hard to do for typically faint high- z sources, and it is thus an area where gravitational lensing magnification helps greatly, as demonstrated in this paper.

In addition to the redshift confirmation, spectroscopy provides information on properties of the interstellar and intergalactic media (ISM and IGM). In particular, Lyman- α emission from sources close to the reionization era is a valuable diagnostic given that it is easily erased by neutral gas within and around galaxies. Its observed strength in distant galaxies is a gauge of the time when reionization was completed (Robertson et al. 2010). Furthermore, we expect Lyman- α Emitters (LAEs) to be predominantly dust-free galaxies; hence their numbers should increase with redshift until the state of the IGM becomes neutral, at which point their numbers should decline.

Significant progress has been made in detecting Lyman- α emitters (LAEs) in narrow band and spectroscopic surveys at $z \gtrsim 6$ (e.g., Kashikawa et al. 2006, Rhoads et al. 2012, Schenker et al. 2012, Clément et al. 2012, Curtis-Lake et al. 2012, Ono et al. 2012, Stark et al. 2011, Pentericci et al. 2011). Most studies see a decline in the LAE population at $z > 7$,

marusa@physics.ucdavis.edu

* Observations were carried out using the Very Large Telescope at the ESO Paranal Observatory under Program ID 088.A-0542. Also based on observations made with the NASA/ESA Hubble Space Telescope, obtained at the Space Telescope Science Institute, which is operated by the Association of Universities for Research in Astronomy, Inc., under NASA contract NAS 5-26555 and NNX08AD79G. These observations are associated with programs # GO10200, GO10863, and GO11099.

¹ Department of Physics, University of California, Davis, CA 95616, USA

² INAF, Osservatorio Astronomico di Trieste, via G.B. Tiepolo 11, 34131 Trieste, Italy

³ Department of Physics, University of California, Santa Barbara, CA 93106, USA

⁴ INAF, Osservatorio Astronomico di Roma, via Frascati 33, 00040 Monteporzio, Italy

⁵ Department of Astronomy, University of Florida, 211 Bryant Space Science Center, Gainesville, FL 32611, USA

⁶ Department of Physics & Astronomy, Ohio University, Clipper Labs 251B, Athens, OH 45701

⁷ Steward Observatory, University of Arizona, 933 N Cherry Ave., Tucson, AZ 85721, USA

⁸ Space Telescope Science Institute, 3700 San Martin Drive, Baltimore, MD 21218, USA

^x Sloan Fellow, Packard Fellow

but not all do (Krug et al. 2012, Tilvi et al. 2010). The declining fraction of LAEs within the LBG population (Stark et al. 2010, Kashikawa et al. 2011, Pentericci et al. 2011) is consistent with this decline being due to changes in the ISM/IGM, specifically to an increased amount of neutral gas. However, current studies only probe the bright end of the luminosity function of LBGs.

Furthermore, as noted by Dijkstra et al. (2011), and Dayal & Ferrara (2012), measuring the rest frame Equivalent Width (EW) distribution of LAEs as a function of redshift *and* luminosity is a powerful tool to study reionization. The EW distribution changes with redshift and source luminosity. Simulations suggest that reionization is the key factor driving this trend (Dayal & Ferrara 2012), because unlike continuum photons, the Lyman- α photons that escape the galactic environment are attenuated by the H I in the IGM. With a measurement of the EW distribution in LAEs we can therefore help distinguish between effects of ISM dust and neutral IGM and study the epoch of reionization (see also Treu et al. 2012). The main missing observational ingredient is a measurement of the EW distribution for both luminous and sub- L^* galaxies at the redshifts of reionization and this can only be achieved with spectroscopy.

Current spectroscopic observations unfortunately fall short of matching the extremely deep near-IR HST/WFC3 data for a significant sample of $z \gtrsim 7$ dropout selected galaxies. Even with state of the art facilities (e.g. the new spectrograph MOSFIRE on Keck, McLean et al. 2010) this will be a challenge. While samples of $\lesssim L^*$ galaxies at $z < 6.5$ is steadily increasing (e.g., Richard et al. 2011, Schenker et al. 2012, Labbé et al. 2010 for spectroscopic and imaging detections), to date, very few $\lesssim L^*$ galaxies at $z \gtrsim 6.5$ are spectroscopically confirmed. The only examples are a lensed $z = 7.045$ galaxy and a marginal detection at $z = 6.905$ by Schenker et al. (2012). At $\sim L^*$ a $z = 6.944$ galaxy was detected by Rhoads et al. (2012). At $z \sim 8$ Lehnert et al. (2010) report a marginal detection of an emission line, but independent observations do not detect it (Bunker et al. 2012, in prep.). Other surveys (Shibuya et al. 2012, Ono et al. 2012, Vanzella et al. 2011, Pentericci et al. 2011, Fontana et al. 2010) target mostly brighter sources. It is important to increase the sample at $z > 6.5$ and compare it to $z < 6.5$ because the timescale for changing the number of LAEs and their observed EW distribution close to the reionization epoch is shorter than the interval of cosmic time between $z \simeq 6$ and $z \simeq 7$ (Dayal & Ferrara 2012).

A powerful way to detect emission lines from faint sources is to use galaxy clusters as cosmic telescopes (e.g. Treu 2010 for a recent review). Gravitational lensing magnifies solid angles while preserving colors and surface brightness. Thus, sources appear brighter than in the absence of lensing. The advantages of cosmic telescopes are that we can probe deeper (due to magnification), sources are practically always enlarged, and identification is further eased if sources are multiply imaged. Typically, one can gain several magnitudes of magnification, thus enabling the study of intrinsically lower-luminosity galaxies that we would otherwise not be able to detect with even the largest telescopes. Indeed the highest redshift sub- L^* LBG currently spectroscopically

confirmed is the $z = 7.045$ galaxy lensed by a cluster A1703 (Schenker et al. 2012). Observations using galaxy clusters as cosmic telescopes are consistently delivering record holders in the search for the highest redshift galaxies (Kneib et al. 2004, Bradley et al. 2008, Zheng et al. 2012). For this reason we have started a large campaign of spectroscopic follow-up of $z > 6.5$ candidates behind the best cosmic telescopes. In this paper we present the first spectroscopic confirmation from this campaign: a $z = 6.740 \pm 0.003$ galaxy behind the Bullet Cluster.

This paper is structured as follows. In Section 2 we describe the data acquisition and reduction, in Section 3 we present the spectrum of the galaxy and we summarize our conclusions in Section 4. Throughout the paper we assume a Λ CDM cosmology with $\Omega_m = 0.3$, $\Omega_\Lambda = 0.7$, and Hubble constant $H_0 = 70 \text{ kms}^{-1} \text{ Mpc}^{-1}$. Coordinates are given for the epoch J2000.0, magnitudes are in the AB system.

2. TARGETS, IMAGING AND SPECTROSCOPIC OBSERVATIONS

Our targets were selected from deep ACS/WFC3 HST observations and are presented by Hall et al. (2012). We targeted all 10 z_{850LP} -band dropouts with the FORS2 spectrograph on the ESO Very Large Telescope, Program ID 088.A-0542 (PI Bradač). Here we present the first detection. The rest of the objects were not detected, inferences obtained from the non-detections and the spectra of filler slits will be presented in a subsequent paper.

The data were taken in service mode during 2011-2012 November-January. We used the 600Z holographic grating providing the highest sensitivity in the spectral range of $8000 - 10000 \text{ \AA}$ with a resolution $R \sim 1390$ and a sampling of $1.6 \text{ \AA pixel}^{-1}$ for a $1'' \times 6''$ slit. The spectra presented here come from the coaddition of 42 exposures of 1400s of integration each, with median seeing around $0''.7$. Series of spectra were taken with two different masks, but all our main targets were placed on both masks for a total integration time of 16.3hr. Standard flat-fielding, bias subtraction, sky subtraction, and wavelength calibration have been applied as in Vanzella et al. (2009, 2011). To perform sky subtraction we fit a polynomial to the partial spectra extracted from the slit just above and below the target and apply the fit to the full spectrum. All the sky-subtracted two-dimensional spectra (of a mask) were coadded in the pixel domain. Finally, spectra were flux calibrated using observations of spectrophotometric standards (Fontana et al. 2010). Slit losses are small, given the extremely compact size of the targets and good seeing conditions, and have been neglected in the subsequent discussion.

Most of the HST imaging data of the object are presented by Hall et al. (2012) and summarized in Table 1. In addition, we have reduced data from GO 11591 (PI Kneib) and do not detect the object in I_{814W} . All $1-\sigma$ limiting magnitudes are given in Table 1. We augment the HST data with imaging data from HAWK-I (Clément et al. 2012). The object is undetected at $3-\sigma$ in the Y, NB1060, J, and K_s bands, which is consistent with our interpretation of the HST detections. For the purpose of determining photometric redshift we only use the HAWK-I non-detection in K_s -band (the other bands overlap with and are shallower than HST detections). The source is also undetected in all four SPITZER IRAC

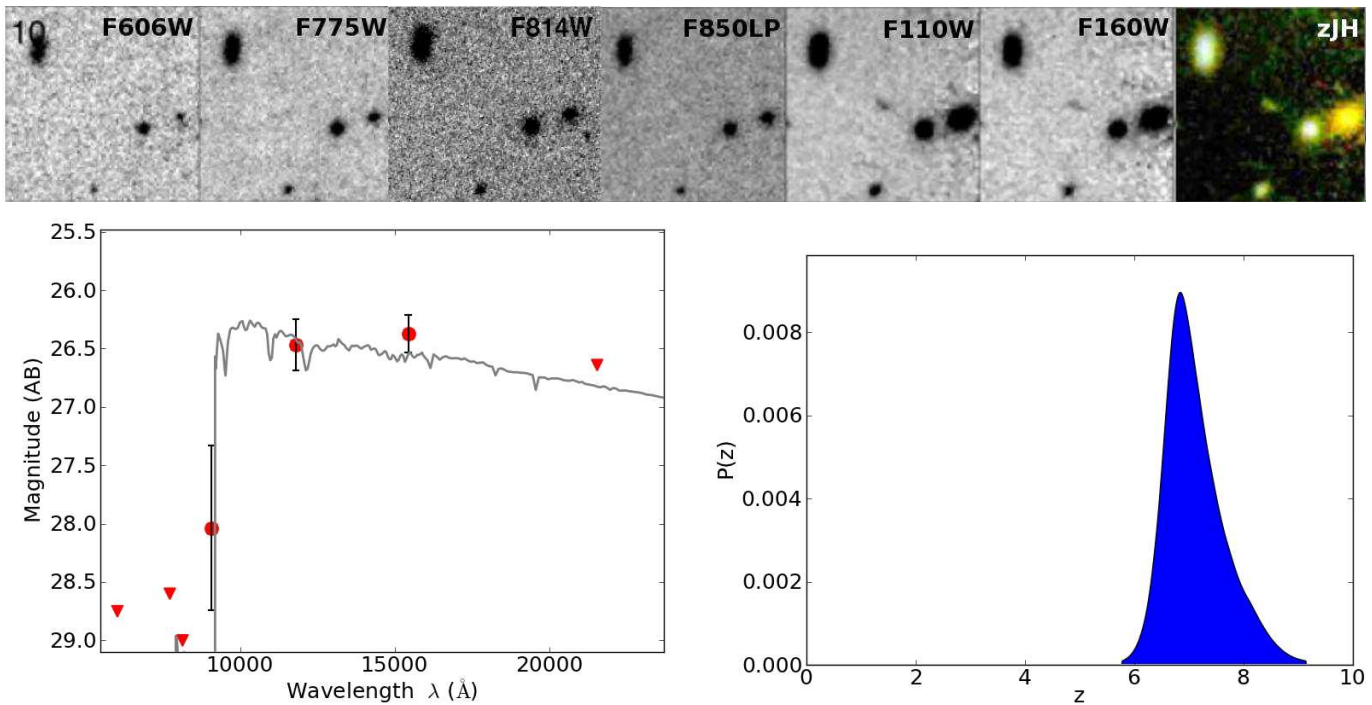


FIG. 1.— (top) Cutouts of the dropout #10 from Hall et al. (2012) shown (from left to right) in V_{606} , i_{775W} , I_{814W} , z_{850LP} , J_{110W} , H_{160W} , $z_{850LP}J_{110W}H_{160W}$ color image (no bluer bands are available at present). The cutouts are $7'' \times 7''$, which corresponds to 20kpc at $z = 6.740$ and magnification $\mu = 3$. (bottom-left) BPZ SED fit to the photometry of the object. The photometric redshift is $z_{\text{phot}} = 6.8^{+1.6}_{-0.8}$ (95% confidence). The circles give the observed AB magnitudes with uncertainties, while the triangles give the $1\text{-}\sigma$ limiting magnitudes in cases of non-detection. (bottom-right) Posterior probability distribution of the photometric redshift. (bottom plots produced using BPZ tools, Coe et al. 2010).

bands ($[3.6\mu\text{m}]$, $[4.5\mu\text{m}]$, $[5.8\mu\text{m}]$, and $[8\mu\text{m}]$) with effective exposure times of 4ks in each filter. This is not surprising given our detection limit for this object is $m_{H_{160W}} - m_{[3.6\mu\text{m}]} = 4$ at $3\text{-}\sigma$. Unfortunately, existing Spitzer images are too shallow to add to the quality of the photometric redshift estimate, and we only use the data listed in Table 1 in the Spectral Energy Distribution (SED) fit (Fig. 1).

For this we use the BPZ code (Benítez 2000) and assume uniform priors on the spectral types and redshift. The observed SED is best fit (reduced $\chi^2 = 0.3$) by a young starburst (5 Myr) galaxy model at $z_{\text{phot}} = 6.8^{+1.6}_{-0.8}$ (95% confidence) which is in excellent agreement with the spectroscopic data presented below (Fig. 2). The probability that the object is at low redshift given the set of templates used by BPZ is zero (Fig. 1-right). Forcing the solution to $z < 5$ the best fit SED is an elliptical galaxy template at $z_{\text{phot}} = 1.4^{+0.7}_{-0.6}$. To further discard the low- z solution would require either extremely deep F475W ($m_{F475W} = 30$), or deeper Spitzer data; neither of which exists for this object. However, the reduced χ^2 of the fit for $z < 5$ increases by a factor of 10 compared to the high redshift solution; in addition the object is unlikely an elliptical galaxy given the presence of an emission line (see below). We therefore conclude that the object is most likely at $z > 5$.

We also performed an independent fit to the photometric data using the HyperZ code (Bolzonella et al. 2000), which has the advantage of treating internal extinction as a free parameter. The results are very similar and the

probability that the object is at high redshift is $> 99\%$. Our conclusions are therefore robust even to cases of heavily reddened, dusty star forming galaxies like the one in (Gonzalez et al. 2010).

Finally, as noted in Hall et al. (2012) it is difficult to estimate the size of the object given the uncertainty in measuring low surface brightness objects. The object is resolved and we estimate the FWHM of $\sim 0''.26$ in J_{110W} and $\sim 0''.21$ in H_{160W} . In physical units and correcting for lensing this translates to $\sim 0.8\text{kpc}$ which is consistent with the compact sizes reported at these high redshifts (e.g., Oesch et al. 2010).

3. RESULTS

The object we present here is the only one for which an emission line was detected, out of the 10 z -band dropout candidates listed in Hall et al. (2012). We detect an emission line at 9412\AA with $> 5\text{-}\sigma$ significance (Figure 2). The line is detected in two different masks and is broader than cosmic rays or residuals due to sky subtraction, hence we are confident that the line is not an artifact. The integrated flux of the line is $f = (0.7 \pm 0.1 \pm 0.3) \times 10^{-17} \text{erg/s/cm}^2$, where the first error corresponds to statistical uncertainty in the detection. The second (larger) is due to systematic uncertainty in absolute flux calibration and due to flux losses in the proximity of skylines and was estimated based on previous multiple observations of various standard stars. No other emission lines are detected in the spectrum ($7700\text{\AA} - 10000\text{\AA}$), which one would expect for some of the possible low- z solutions as discussed below. Based

TABLE 1
IMAGING AND SPECTROSCOPIC PROPERTIES OF Z₈₅₀-BAND DROPOUT
10 FROM HALL ET AL. (2012)

R.A.	104.63015
Dec.	-55.970482
$m_{H_{160W}}$	26.37 ± 0.16
$m_{J_{110W}}$	26.5 ± 0.3
$(J_{110W} - H_{160W})$	0.10 ± 0.15
$(z_{850LP} - J_{110W})$	1.57 ± 0.68
$m_{V_{606}}^{(a)}$	> 28.75 ($t_{exp} = 2336s$)
$m_{i_{775W}}$	> 28.60 ($t_{exp} = 10150s$)
$m_{i_{814W}}$	> 29.00 ($t_{exp} = 4480s$)
m_{K_s}	> 26.65 ($t_{exp} = 3.75hr$)
μ	3.0 ± 0.2
$m_{H_{160W}}^{int}$	$27.57^{+0.17}_{-0.17}$
λ	9412Å
z	6.740 ± 0.003
$f^{(b)}$	$(0.7 \pm 0.1 \pm 0.3) \times 10^{-17} \text{ erg/s/cm}^2$
$f_{\lambda,c}$	$3.3^{+1.0}_{-0.8} \times 10^{-20} \text{ erg/s/cm}^2/\text{Å}$
f^{int}	$(0.23 \pm 0.03 \pm 0.10 \pm 0.02) \times 10^{-17} \text{ erg/s/cm}^2$
$f_{\lambda,c}^{int}$	$1.1^{+0.4}_{-0.3} \times 10^{-20} \text{ erg/s/cm}^2/\text{Å}$
$W^{rest}(\text{Ly}\alpha)$	30^{+12}_{-21} Å

(a) All upper limits are $1-\sigma$ limiting magnitudes calculated in $0.63'' \times 0.63''$ square apertures. t_{exp} is the exposure time in corresponding band.

(b) f is the integrated line flux, $f_{\lambda,c}$ is the continuum flux estimated from the J_{110W} magnitude, while int denotes corresponding intrinsic (unlensed) values.

on this and on the SED fit we exclude other alternative explanations and conclude that the line is most likely Lyman- α at $z = 6.740 \pm 0.003$. This agrees extremely well with the peak redshift probability distribution described in Sect. 2.

Because of the relatively low signal-to-noise ratio of the spectrum we cannot determine whether the line is asymmetric (which is expected for high redshift LAEs where absorption happens mostly in the blue wing of the line) and thus further test our identification as Lyman- α . However, we use indirect arguments to test the alternative hypothesis that this galaxy is at a low redshift and the line is not Lyman- α but: (1) [O II] (3727Å) at $z = 1.525$; (2) [O III] (4959Å, 5007Å) at $z = 0.898, 0.880$; or (3) H- α (6563Å) at $z = 0.434$, which are the prominent lines in emission line galaxies (e.g., Straughn et al. 2009).

(1) Any of the three low redshift scenarios are strongly disfavored by photometry. As shown in Figure 3-right, the fit to the photometric data while forcing $z < 5$ is very poor ($z_{phot} = 1.4^{+0.7}_{-0.6}$). Forcing it to $z = 1.525$ (if line is [O II]), or accounting for the emission due to the line, does not change the quality of the fit. The [O II] doublet should nominally be resolved at our resolution; however the sky emission at these wavelengths degrades S/N and our ability to distinguish individual components (Fig 3-left). Unfortunately, in either scenario (Lyman- α /[O II]) no other lines are expected in the wavelength range covered by the spectrum (7700Å – 10000Å). The line has the rest frame EW of $\sim 100\text{Å}$ if at $z = 1.5$ ([O II] scenario) and $\sim 150\text{Å}$ if at $z = 0.43$ (H- α). This is higher than typical [O II], and H- α emitters equivalent widths as measured by Straughn et al. (2009). Their median equivalent widths are 36Å and 73Å for [O II] and H- α respectively. Out of 30 [O II] emitters only 3 have equiv-

alent width $> 100\text{Å}$. Hence, given the photometry and strength of the line we conclude that the [O II] scenario is very unlikely.

(2) [O III] at $z = 0.880$ is even more strongly disfavored as we would expect to detect the second line of [O III] as well as H- β line for typical line ratios. That part of the spectra is clear, hence this identification is ruled out by the data. (3) H- α at $z = 0.434$ is also strongly disfavored by the photometry.

Recently Hayes et al. (2012) cautioned against using photometry only to select high redshift galaxies. They targeted a J_{110W} -band dropout from Laporte et al. (2011) and discovered it was a low redshift interloper. However, their situation is different from the one reported here. While their target is a J_{110W} -band dropout by their selection criteria, the object is detected blueward of Lyman- α in the i_{775W} -band and the resulting best-fit model is poor. Even without the i_{775W} -band observations the photometry can be fit with a low- z template. In our case the high redshift SED fit is good and the low redshift fit is extremely poor.

We conclude that the line is most likely Lyman- α at $z = 6.740 \pm 0.003$. The object has an AB magnitude of 26.5 ± 0.3 in the J_{110W} -band (lensed, before correcting for magnification), which corresponds to a continuum flux of $f_{\lambda,c} = 3.3^{+1.0}_{-0.8} \times 10^{-20} \text{ erg/s/cm}^2/\text{Å}$. With an integrated line flux of $f = (0.7 \pm 0.1 \pm 0.3) \times 10^{-17} \text{ erg/s/cm}^2$, the resulting line rest-frame equivalent width is $W^{rest}(\text{Ly}\alpha) = f/f_{\lambda,c}(1+z) = 30^{+12}_{-21} \text{ Å}$ (Table 1). The distribution of EW (including non-detections) of the total sample of 10 dropouts to be presented in a future paper will help distinguish between scenarios of Lyman- α opacity around the epoch of reionization (Treu et al. 2012).

Using the data we also obtain rough estimate for the star formation rates (SFRs) using both Lyman- α and UV continuum luminosities, and Kennicutt's relations (Kennicutt 1998). We first estimate the SFR from the Lyman- α luminosity $L_{\text{Ly}\alpha}$ for the case B recombination theory as $SFR_{\text{Ly}\alpha} = 9.1 \times L_{\text{Ly}\alpha} [M_{\odot}/\text{yr}]$, with $L_{\text{Ly}\alpha}$ in units of $10^{43} \text{ erg s}^{-1}$. We obtain $SFR \sim (3.3 \pm 1.5)/\mu M_{\odot}/\text{yr}$, where errors only include measurement errors on $L_{\text{Ly}\alpha}$ and no uncertainties in Kennicutt's relation. Note that this is a lower limit since $L_{\text{Ly}\alpha}$ is not corrected for absorption effects which depend on various parameters, including the neutral fraction of the IGM and the kinematic status of neutral hydrogen.

To convert UV luminosity L_{UV} into SFR we use $SFR_{\text{UV}} = 1.4 \times L_{\text{UV}} [M_{\odot}/\text{yr}]$, where L_{UV} is in units of $10^{28} \text{ erg s}^{-1} \text{ Hz}^{-1}$. We estimate $L_{\text{UV}} = (6.2^{+1.8}_{-1.5}) 10^{28} \text{ erg s}^{-1} \text{ Hz}^{-1}$ using J_{110W} -band magnitude, as the central wavelength is very close to rest-frame 1500Å , giving $SFR_{\text{UV}} = 8.7^{+2.6}_{-2.1}/\mu M_{\odot}/\text{yr}$. Both estimates are fully compatible within systematic and statistical uncertainties implying that the dust attenuation is very low (Verhamme et al. 2008), which is also indicated by the blue UV spectral slope from J_{110W}, H_{160W} and K_s band photometry. Dividing SFR by magnification, the intrinsic star formation rate is $SFR \sim 2 - 3 M_{\odot}/\text{yr}$, consistent with SFR from, e.g., Labbé et al. (2010).

4. CONCLUSION

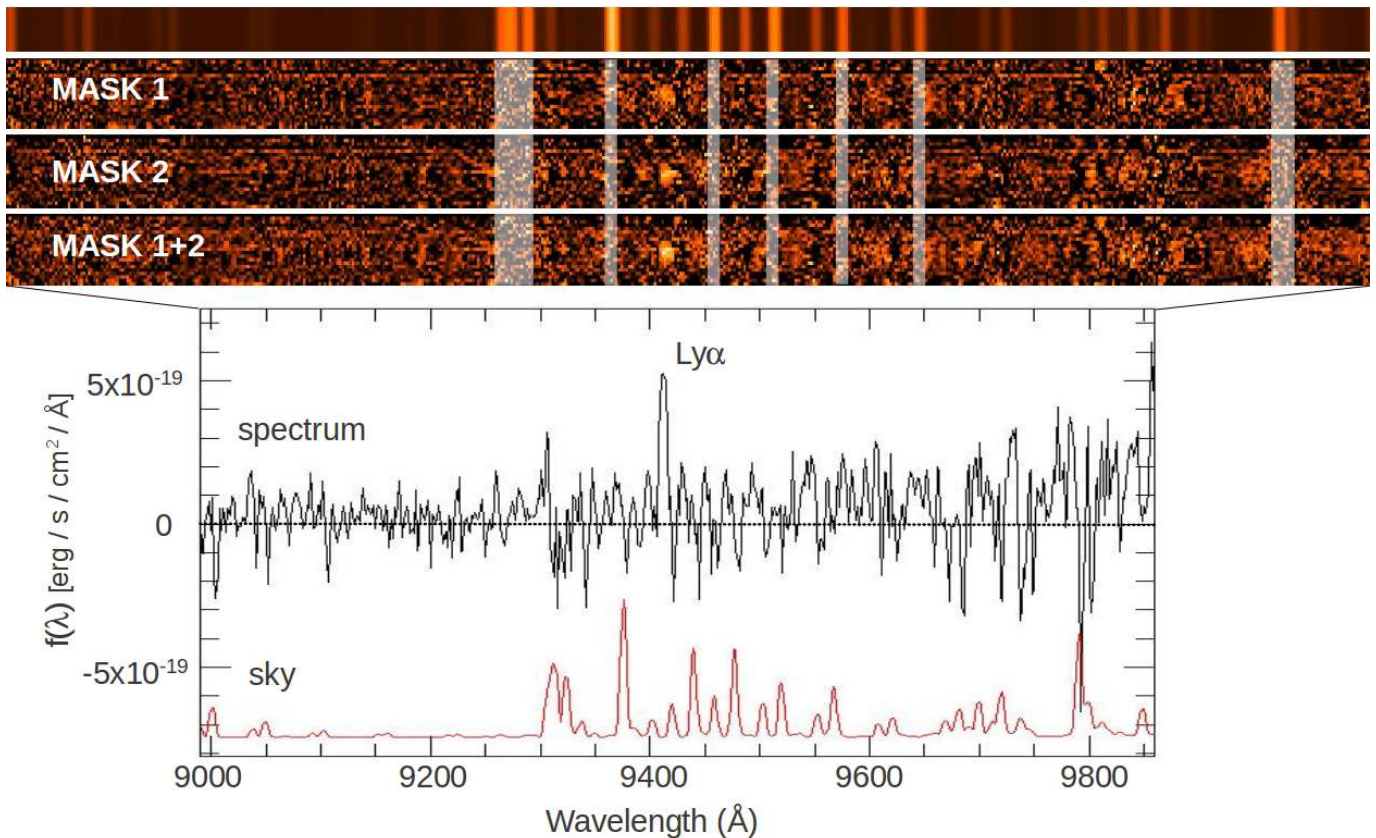


FIG. 2.— (top) 2-D spectrum of the dropout galaxy (sky emission above, spectra from individual masks below). (bottom) 1-D spectrum of the object. The sky spectrum has been rescaled by a factor of 300 and offset for plot purposes, and the regions where skylines are more intense have been marked with transparent vertical bars. Strong residuals in the sky subtraction are evident and correspond to the more intense sky lines. Note that the detected line is broader than residuals of sky subtraction, confirming the reality of the feature.

We have presented deep VLT spectroscopy of a strongly lensed $z_{850\text{LP}}$ -band dropout galaxy behind the Bullet cluster. We detected an emission line at 9412\AA with $> 5\text{-}\sigma$ significance, which we identify as Lyman- α at $z = 6.740 \pm 0.003$ at $> 99\%\text{CL}$. Correcting for magnification (by a factor of $\mu = 3.0 \pm 0.2$ as discussed by Hall et al. 2012, Bradač et al. 2009), the intrinsic (unlensed) line flux is $f = (0.23 \pm 0.03 \pm 0.10 \pm 0.02) \times 10^{-17} \text{erg/s/cm}^2$ (Table 1), which is $\sim 2 - 3$ times fainter than the faintest spectroscopic detection of an LAE at $z \sim 7$ (Schenker et al. 2012). Its intrinsic $H_{160\text{W}}$ -band magnitude is $m_{H_{160\text{W}}}^{\text{int}} = 27.57 \pm 0.17$, corresponding to an intrinsic luminosity of $0.5L^*$ (where L^* was calculated from the best fit LBG luminosity function from Bouwens et al. 2011).

The source is undetected in the four IRAC bands, which is not surprising given that we would only be able to detect extremely red galaxies with $m_{H_{160\text{W}}} - m_{[3.6\mu\text{m}]} = 4$ at $3\text{-}\sigma$ in $[3.6\mu\text{m}]$ for sources this faint. For comparison, $z = 6.027$ source behind A383 (Richard et al. 2011) with an unusually mature stellar population $\sim 800\text{Myr}$ and a multiply-imaged $z = 6.2$ object (Zitrin et al. 2012) with a younger age $\sim 180\text{Myr}$ have much bluer colors $m_{H_{160\text{W}}} - m_{[3.6\mu\text{m}]} \sim 1.5$. Deeper Spitzer data will be needed to probe the presence of mature stellar populations in the galaxy we present here and other systems at high redshift.

While this work presents only a single spectroscopic de-

tection at $z > 6.5$, it nonetheless probes a very important region of parameter space. As noted above, measuring the EW distribution of LAEs as a function of redshift *and* luminosity is a very powerful tool to study reionization, because the latter is likely the key factor driving the trend of EW in luminosity (Dayal & Ferrara 2012). The main missing observational ingredient is a measurement of the EW distribution for both luminous and sub- L^* galaxies at the redshifts of reionization.

Our source is the faintest one (in line flux) detected thus far and is only the second firm spectroscopic detection of a sub- L^* source at $z > 6.5$. With future observations of dropouts magnified by cosmic telescopes we plan to further increase this sample. Once completed, this survey will help constrain the duration and physical processes occurring at the epoch of reionization.

We would like to thank the anonymous referee for suggestions that greatly improved the paper and Sam Schmidt, Michele Trenti, and Andy Bunker for stimulating discussions. Support for this work was provided by NASA through HST-GO-10200, HST-GO-10863, and HST-GO-11099 from STScI. EV acknowledges financial contribution from ASI-INAF I/009/10/0 and PRIN MIUR 2009 “Tracing the growth of structures in the Universe: from the high-redshift cosmic web to galaxy clusters”. TT acknowledges support from the NSF through CAREER/NSF-0642621, through a Sloan Research Fel-

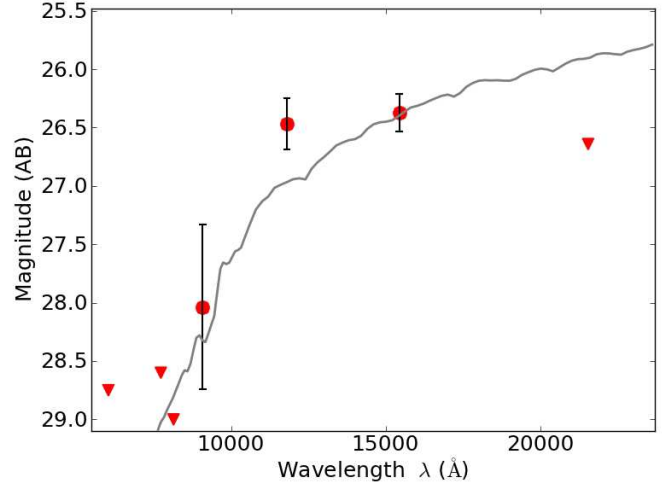
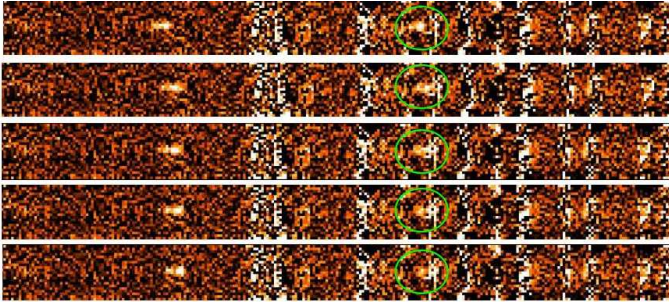


FIG. 3.— (left) Tests of a possible [O II] line interpretation. An [O II] line from another spectrum has been degraded to the S/N of our detected line and placed at slightly different wavelengths and in two different regions in an empty slit (around 9412Å and in a place with fewer skylines for comparison). Due to the low S/N and the proximity of skylines we can not fully rule out the possibility of the line being an [O II] based on this test *alone*. (right) Best fit SED when forcing the redshift to be $z < 5$. Labels are as in Fig. 1. The favored solution is at $z_{\text{phot}} = 1.4_{-0.6}^{+0.7}$ albeit with a very poor fit.

lowship, and by the Packard Fellowship. Part of the work was carried out by MB and TT while attending the program "First Galaxies and Faint Dwarfs" at KITP which

is supported in part by the NSF under Grant No. NSF PHY11-25915.

REFERENCES

- Benítez, N. 2000, *ApJ*, 536, 571
- Bolzonella, M., Miralles, J.-M., & Pelló, R. 2000, *A&A*, 363, 476
- Bouwens, R. J., Illingworth, G. D., Oesch, P. A., Labbé, I., Trenti, M., van Dokkum, P., Franx, M., Stiavelli, M., Carollo, C. M., Magee, D., & Gonzalez, V. 2011, *ApJ*, 737, 90
- Bouwens, R. J., Illingworth, G. D., Oesch, P. A., Trenti, M., Labbé, I., Franx, M., Stiavelli, M., Carollo, C. M., van Dokkum, P., & Magee, D. 2012, *ApJ*, 752, L5
- Bradač, M., Treu, T., Applegate, D., Gonzalez, A. H., Clowe, D., Forman, W., Jones, C., Marshall, P., Schneider, P., & Zaritsky, D. 2009, *ApJ*, 706, 1201
- Bradley, L. D., Bouwens, R. J., Ford, H. C., Illingworth, G. D., Jee, M. J., Benítez, N., Broadhurst, T. J., Franx, M., Frye, B. L., Infante, L., Motta, V., Rosati, P., White, R. L., & Zheng, W. 2008, *ApJ*, 678, 647
- Bradley, L. D., Bouwens, R. J., Zitrin, A., Smit, R., Coe, D., Ford, H. C., Zheng, W., Illingworth, G. D., Benítez, N., & Broadhurst, T. J. 2012, *ApJ*, 747, 3
- Bunker, A. J., Caruana, J., Wilkin, S., Stanway, E., Lorenzoni, S., Lacy, M., Jarvis, M., & Hickey, S. 2012, in prep.
- Clément, B., Cuby, J.-G., Courbin, F., Fontana, A., Freudling, W., Fynbo, J., Gallego, J., Hibon, P., Kneib, J.-P., Le Fèvre, O., Lidman, C., McMahon, R., Milvang-Jensen, B., Moller, P., Moorwood, A., Nilsson, K. K., Pentericci, L., Venemans, B., Villar, V., & Willis, J. 2012, *A&A*, 538, A66
- Coe, D., Benítez, N., Broadhurst, T., & Moustakas, L. A. 2010, *ApJ*, 723, 1678
- Curtis-Lake, E., McLure, R. J., Pearce, H. J., Dunlop, J. S., Cirasuolo, M., Stark, D. P., Almaini, O., Bradshaw, E. J., Chuter, R., Foucaud, S., & Hartley, W. G. 2012, *MNRAS*, 422, 1425
- Dayal, P. & Ferrara, A. 2012, *MNRAS*, 421, 2568
- Dijkstra, M., Mesinger, A., & Wyithe, J. S. B. 2011, *MNRAS*, 414, 2139
- Egami, E., Kneib, J.-P., Rieke, G. H., Ellis, R. S., Richard, J., Rigby, J., Papovich, C., Stark, D., Santos, M. R., Huang, J.-S., Dole, H., Le Flocc'h, E., & Pérez-González, P. G. 2005, *ApJ*, 618, L5
- Finkelstein, S. L., Papovich, C., Ryan, Jr., R. E., Pawlik, A. H., Dickinson, M., Ferguson, H. C., Finlator, K., Koekemoer, A. M., Giavalisco, M., Cooray, A., Dunlop, J. S., Faber, S. M., Grogin, N. A., Kocevski, D. D., & Newman, J. A. 2012, arXiv:1206.0735
- Fontana, A., Vanzella, E., Pentericci, L., Castellano, M., Giavalisco, M., Grazian, A., Boutsia, K., Cristiani, S., Dickinson, M., Giallongo, E., Maiolino, R., Moorwood, A., & Santini, P. 2010, *ApJ*, 725, L205
- Gonzalez, A. H., Papovich, C., Bradač, M., & Jones, C. 2010, *ApJ*, 720, 245
- Hall, N., Bradač, M., Gonzalez, A. H., Treu, T., Clowe, D., Jones, C., Stiavelli, M., Zaritsky, D., Cuby, J.-G., & Clément, B. 2012, *ApJ*, 745, 155
- Hayes, M., Laporte, N., Pello, R., Schaerer, D., & Le Borgne, J.-F. 2012, arXiv:1205.6815
- Kashikawa, N., Shimasaku, K., Malkan, M. A., Doi, M., Matsuda, Y., Ouchi, M., Taniguchi, Y., Ly, C., Nagao, T., Iye, M., Motohara, K., Murayama, T., Murozono, K., Nariai, K., Ohta, K., Okamura, S., Sasaki, T., Shioya, Y., & Umemura, M. 2006, *ApJ*, 648, 7
- Kashikawa, N., Shimasaku, K., Matsuda, Y., Egami, E., Jiang, L., Nagao, T., Ouchi, M., Malkan, M. A., Hattori, T., Ota, K., Taniguchi, Y., Okamura, S., Ly, C., Iye, M., Furusawa, H., Shioya, Y., Shibuya, T., Ishizaki, Y., & Toshikawa, J. 2011, *ApJ*, 734, 119
- Kennicutt, Jr., R. C. 1998, *ApJ*, 498, 541
- Kneib, J., Ellis, R. S., Santos, M. R., & Richard, J. 2004, *ApJ*, 607, 697
- Krug, H. B., Veilleux, S., Tilvi, V., Malhotra, S., Rhoads, J., Hibon, P., Swaters, R., Probst, R., Dey, A., Dickinson, M., & Jannuzi, B. T. 2012, *ApJ*, 745, 122
- Labbé, I., González, V., Bouwens, R. J., Illingworth, G. D., Oesch, P. A., van Dokkum, P. G., Carollo, C. M., Franx, M., Stiavelli, M., Trenti, M., Magee, D., & Kriek, M. 2010, *ApJ*, 708, L26
- Laporte, N., Pelló, R., Schaerer, D., Richard, J., Egami, E., Kneib, J. P., Le Borgne, J. F., Maizy, A., Boone, F., Hudelot, P., & Mellier, Y. 2011, *A&A*, 531, A74
- Lehnert, M. D., Nesvadba, N. P. H., Cuby, J., Swinbank, A. M., Morris, S., Clément, B., Evans, C. J., Bremer, M. N., & Basa, S. 2010, *Nature*, 467, 940

- McLean, I. S., Steidel, C. C., Epps, H., Matthews, K., Adkins, S., Konidaris, N., Weber, B., Aliado, T., Brims, G., Canfield, J., Cromer, J., Fucik, J., Kulas, K., Mace, G., Magnone, K., Rodriguez, H., Wang, E., & Weiss, J. 2010, in *Society of Photo-Optical Instrumentation Engineers (SPIE) Conference Series*, Vol. 7735, *Society of Photo-Optical Instrumentation Engineers (SPIE) Conference Series*
- McLure, R. J., Dunlop, J. S., de Ravel, L., Cirasuolo, M., Ellis, R. S., Schenker, M., Robertson, B. E., Koekemoer, A. M., Stark, D. P., & Bowler, R. A. A. 2011, *MNRAS*, 418, 2074
- Oesch, P. A., Bouwens, R. J., Carollo, C. M., Illingworth, G. D., Trenti, M., Stiavelli, M., Magee, D., Labbé, I., & Franx, M. 2010, *ApJ*, 709, L21
- Oesch, P. A., Bouwens, R. J., Illingworth, G. D., Labbé, I., Trenti, M., Gonzalez, V., Carollo, C. M., Franx, M., van Dokkum, P. G., & Magee, D. 2012, *ApJ*, 745, 110
- Ono, Y., Ouchi, M., Mobasher, B., Dickinson, M., Penner, K., Shimasaku, K., Weiner, B. J., Kartaltepe, J. S., Nakajima, K., Nayyeri, H., Stern, D., Kashikawa, N., & Spinrad, H. 2012, *ApJ*, 744, 83
- Pentericci, L., Fontana, A., Vanzella, E., Castellano, M., Grazian, A., Dijkstra, M., Boutsia, K., Cristiani, S., Dickinson, M., Giallongo, E., Giavalisco, M., Maiolino, R., Moorwood, A., Paris, D., & Santini, P. 2011, *ApJ*, 743, 132
- Rhoads, J. E., Hiben, P., Malhotra, S., Cooper, M., & Weiner, B. 2012, *arXiv:1205.3161*
- Richard, J., Kneib, J.-P., Ebeling, H., Stark, D. P., Egami, E., & Fiedler, A. K. 2011, *MNRAS*, 414, L31
- Robertson, B. E., Ellis, R. S., Dunlop, J. S., McLure, R. J., & Stark, D. P. 2010, *Nature*, 468, 49
- Schenker, M. A., Stark, D. P., Ellis, R. S., Robertson, B. E., Dunlop, J. S., McLure, R. J., Kneib, J.-P., & Richard, J. 2012, *ApJ*, 744, 179
- Shibuya, T., Kashikawa, N., Ota, K., Iye, M., Ouchi, M., Furusawa, H., Shimasaku, K., & Hattori, T. 2012, *ApJ*, 752, 114
- Stark, D. P., Ellis, R. S., Chiu, K., Ouchi, M., & Bunker, A. 2010, *MNRAS*, 408, 1628
- Stark, D. P., Ellis, R. S., & Ouchi, M. 2011, *ApJ*, 728, L2+
- Steidel, C. C., Giavalisco, M., Pettini, M., Dickinson, M., & Adelberger, K. L. 1996, *ApJ*, 462, L17+
- Straughn, A. N., Pirzkal, N., Meurer, G. R., Cohen, S. H., Windhorst, R. A., Malhotra, S., Rhoads, J., Gardner, J. P., Hathi, N. P., Jansen, R. A., Grogin, N., Panagia, N., di Serego Alighieri, S., Gronwall, C., Walsh, J., Pasquali, A., & Xu, C. 2009, *AJ*, 138, 1022
- Tilvi, V., Rhoads, J. E., Hiben, P., Malhotra, S., Wang, J., Veilleux, S., Swaters, R., Probst, R., Krug, H., Finkelstein, S. L., & Dickinson, M. 2010, *ApJ*, 721, 1853
- Treu, T. 2010, *ARA&A*, 48, 87
- Treu, T., Trenti, M., Stiavelli, M., Auger, M. W., & Bradley, L. D. 2012, *ApJ*, 747, 27
- Vanzella, E., Giavalisco, M., Dickinson, M., Cristiani, S., Nonino, M., Kuntschner, H., Popesso, P., Rosati, P., Renzini, A., Stern, D., Cesarsky, C., Ferguson, H. C., & Fosbury, R. A. E. 2009, *ApJ*, 695, 1163
- Vanzella, E., Pentericci, L., Fontana, A., Grazian, A., Castellano, M., Boutsia, K., Cristiani, S., Dickinson, M., Gallozzi, S., Giallongo, E., Giavalisco, M., Maiolino, R., Moorwood, A., Paris, D., & Santini, P. 2011, *ApJ*, 730, L35
- Verhamme, A., Schaerer, D., Atek, H., & Tapken, C. 2008, *A&A*, 491, 89
- Zheng, W., Postman, M., Zitrin, A., Moustakas, J., Shu, X., Jouvel, S., Host, O., Molino, A., Bradley, L., Coe, D., Moustakas, L. A., Carrasco, M., Ford, H., Benitez, N., Lauer, T. R., Seitz, S., Bouwens, R., Koekemoer, A., Medezinski, E., Bartelmann, M., Broadhurst, T., Donahue, M., Grillo, C., Infante, L., Jha, S., Kelson, D. D., Lahav, O., Lemze, D., Melchior, P., Meneghetti, M., Merten, J., Nonino, M., Ogaz, S., Rosati, P., Umetsu, K., & van der Wel, A. 2012, *arXiv:1204.2305*
- Zitrin, A., Moustakas, J., Bradley, L., Coe, D., Moustakas, L. A., Postman, M., Shu, X., Zheng, W., Benítez, N., Bouwens, R., Broadhurst, T., Ford, H., Host, O., Jouvel, S., Koekemoer, A., Meneghetti, M., Rosati, P., Donahue, M., Grillo, C., Kelson, D., Lemze, D., Medezinski, E., Molino, A., Nonino, M., & Ogaz, S. 2012, *ApJ*, 747, L9